ELSEVIER

Journal of Crystal Growth 237–239 (2002) 2076–2081

JOURNAL OF CRYSTAL GROWTH

www.elsevier.com/locate/jcrysgro

Structural relationship between epitaxially grown para-sexiphenyl and mica (0 0 1) substrates

H. Plank[a,*], R. Resel[a], A. Andreev[b], N.S. Sariciftci[b], H. Sitter[c]

[a] *Institute for Solid State Physics, Graz University of Technology, Petersgasse 16, 8010, Graz, Austria*
[b] *Institute for Physical Chemistry, University of Linz, Austria*
[c] *Institute for Semiconductor- and Solid State Physics, University of Linz, Austria*

Abstract

This study focuses on structural properties of para-sexiphenyl (PSP) epitaxial thin films grown on freshly cleaved mica (0 0 1) substrates. The layers were prepared by hot wall epitaxy (HWE) technique resulting in highly ordered organic structures with a needle-like morphology on the substrates. X-ray diffraction (XRD) pole figure technique, transmission electron diffraction (TED) and atomic force microscopy were used to characterise the epitaxial growth. However, on not perfectly cleaved mica substrates the needle direction can change around 120° when the films are grown on different terraces of mica (0 0 1) which are separated by cleavage steps. This behaviour can be referred to the properties of the monoclinic crystal structure of mica which is described in detail.

Keywords: A1. Crystal morphology; A1. X-ray diffraction; A3. Hot wall epitaxy

1. Introduction

Para-sexiphenyl (PSP) is a very promising organic semiconducting material for various opto-electronic applications such as polarised light emitting devices [1]. The successful application of the organic films in such devices is strongly dependent on the orientation of the organic molecules within the thin films [2]. Therefore, the detailed characterisation of PSP films is essential for further development. In the present study we consider the structural properties of PSP crystallites epitaxially grown on freshly cleaved mica (0 0 1).

*Corresponding author. Tel.: +43-316-873-8469; fax: +43-3168738478 or 8466.

E-mail address: harald.plank@tugraz.at (H. Plank).

2. Experimental procedure

The PSP films were prepared by hot wall epitaxy (HWE) using freshly cleaved mica as substrate. The PSP material was evaporated at 240°C at a vacuum of about 6×10^{-6} mbar and the substrate temperature was held at 90°C. The growth time of the investigated sample was set to 60 min in order to obtain sufficiently thick films for X-ray investigations [3,4].

The film morphology was investigated with atomic force microscopy (AFM) using a Nano-Scope instrument in a contact mode.

X-ray diffraction pole figure (XRD-PF) measurements were employed with a Philips X'pert system equipped with an ATC3 texture cradle. A Cr K_α tube was used together with a flat graphite

0022-0248/02/$ - see front matter
PII: S0022-0248(01)02313-2

monochromator in Schultz reflection geometry. Pole figures were measured with a ψ limit of 75° and comparable wide open slits [5]. Crystallographic analyses are performed with the software package Powder Cell 2.3 [6] using single crystal data of the β-phase of PSP [7].

The detailed characterisation of the epitaxial growth of PSP on mica (0 0 1) is reported in Ref. [5]. This study, hence, focuses on the detailed structural relations between PSP and mica (0 0 1) in order to interpret the observed growth.

3. Experimental results and discussion

Transmission electron diffraction (TED) confirms the XRD results and enables the determination of the needle direction with respect to the PSP molecules.

3.1. Films on perfectly cleaved mica substrates

The results are highly ordered organic, thin films which show a needle-like morphology of PSP crystallites. On perfectly cleaved mica—without any cleavage steps on the surface—the needles are aligned in a single direction. Fig. 1 shows an AFM image of the investigated sample. AFM line scans

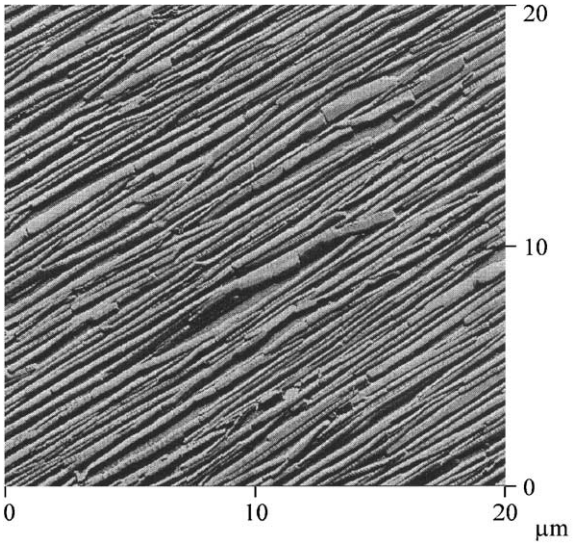

Fig. 1. $20 \times 20\,\mu m^2$ AFM image of PSP on mica (0 0 1).

reveal typical needle widths, heights and lengths of about 800, 130 and 100 μm [3,4].

Fig. 2 shows the XRD pole figures taken from the corresponding 2Θ angles of the four strongest reflections of PSP—(1 1 $\bar{1}$), (1 1 $\bar{2}$), (2 0 $\bar{3}$) and (2 1 $\bar{3}$). The pole figures as well as additional measurements with a 2D area detector reveal a clear epitaxial growth of PSP crystallites on mica (0 0 1). The detailed analysis of the pole figures reveals the crystallographic (1 1 $\bar{1}$) plane of PSP parallel to the substrate surface [5]. Fig. 3 displays the relative molecule arrangement of PSP with respect to the mica (0 0 1) surface. The long axes of PSP molecules are tilted about 4.5° against mica (0 0 1). The molecular planes of the adjacent PSP molecules are tilted about 66° relative to each other, which generates the typical herringbone structure of PSP. However, the long molecular axes of adjacent molecules are aligned parallel. The interface plane of PSP crystallites is also a cleavage plane—which can be seen by Fig. 2a and b—which provides a stable growth of crystallites on the surface.

As is visible in Fig. 2b, not each PSP molecule contacts the substrate surface, hence, for the first investigation it is sufficient to consider only the molecules with perpendicularly oriented molecular planes. Moreover, as is evident in Fig. 2a, only single atoms of the PSP molecules—in the present case hydrogen atoms—interact with the mica surface. The distance between adjacent contacting hydrogen atoms is found to be 9.82 Å in parallel view (Fig. 2b). In the side view (Fig. 2a), the distance between two neighbouring contact point atoms is determined to be 26.34 Å. These contact atoms generate a contact point lattice where the PSP crystallites interact with the mica substrate. In Fig. 4 the generated point lattice of PSP is matched with the correctly oriented mica substrate. The contact points of PSP are indicated by filled circles, whereas the hexagons represent the idealised mica (0 0 1) surface. The inserted distances in Fig. 4 represents the spacings between the contact atoms (also indicated in Fig. 2). Transmission electron microscopy in conjunction with transmission electron diffraction measurements—with the detailed description in Ref. [5]—enables a determination of the needle

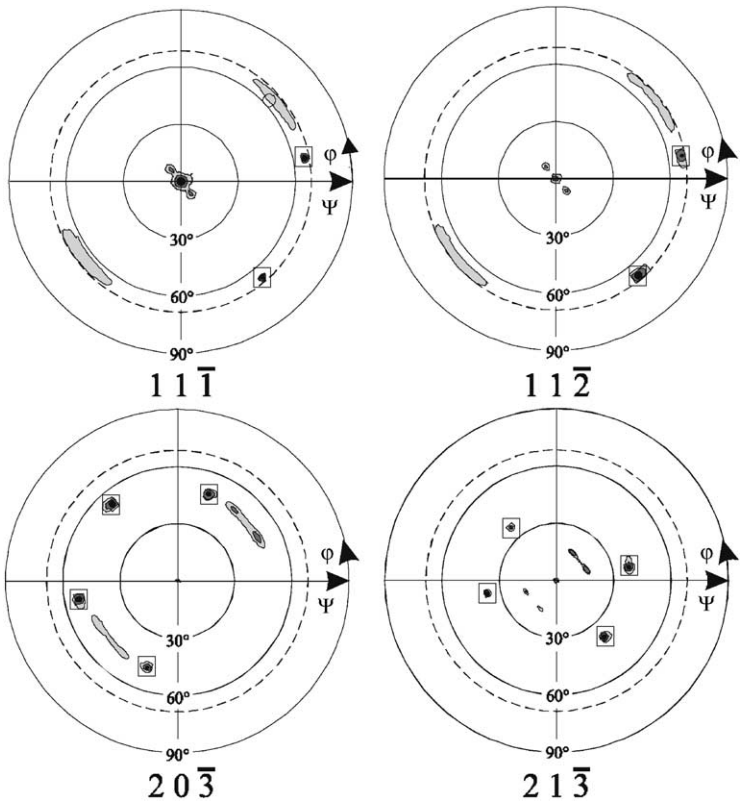

Fig. 2. XRD-PF of PSP on mica (0 0 1). The four pole figures are taken from the (1 1 $\bar{1}$), (1 1 $\bar{2}$), (2 0 $\bar{3}$) and (2 1 $\bar{3}$) reflections of PSP. The dashed line indicates the measurement limit of $\psi = 75°$. Darker areas represent higher intensity.

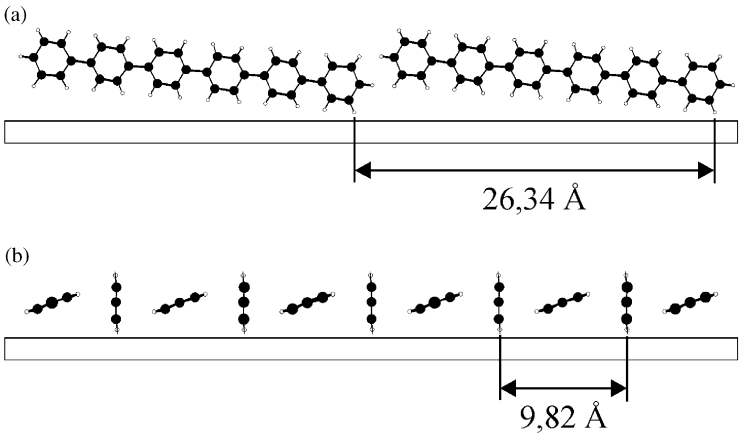

Fig. 3. Arrangement of PSP molecules in a view parallel to the crystallographic (0 0 1) of mica. Two molecules are shown in a side view (a); eleven molecules are given in a parallel view along the molecular planes (b).

direction of the PSP crystallites which is displayed as a dashed line in Fig. 4 with an accuracy of $\pm 5°$ due to the insecurity of defining a needle axis. Since the point lattice of PSP is incommensurate with the surface mesh of mica (0 0 1), we can refer the confirmed epitaxy to quasi-epitaxy [8].

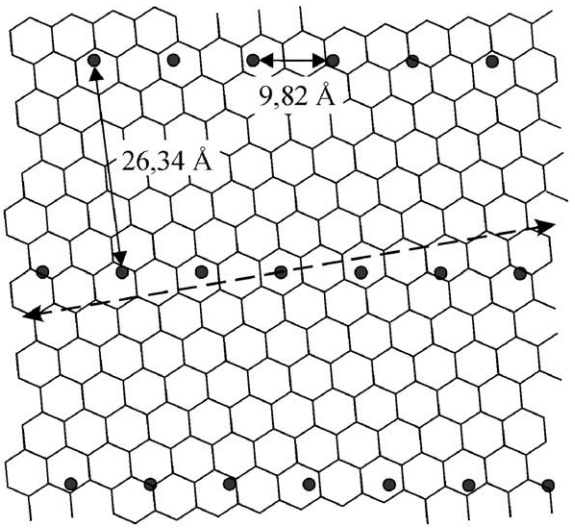

Fig. 4. Contact point lattice—represented by filled circles—of PSP crystallites on an idealised hexagonal mica surface. The dashed line indicates the direction of the needles.

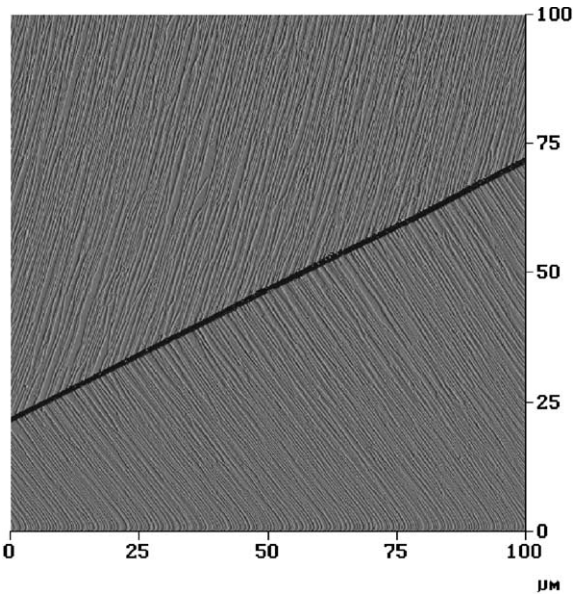

Fig. 5. $100 \times 100\,\mu m^2$ AFM image of PSP grown on two terraces of mica separated by a cleavage step.

A small tilt of the long molecular axes relative to the mica surface—instead of a parallel or vertical alignment—is an unusual case of molecular alignment on surfaces. This behaviour can be explained by the fact that the crystallographic contact plane of PSP crystallites is a cleavage plane of PSP. The observed cleavage plane of PSP in conjunction with the incommensurable interface lattices reveals that the interactions between PSP molecules are dominant—in comparison with the interactions between PSP and mica—for the formation of the epitaxial growth.

3.2. Films on not perfectly cleaved mica substrates

Not perfectly cleaved substrates lead to terraces on the mica surface, separated by big cleavage steps. PSP films which are prepared on such substrates can also change their morphology. From terrace to terrace the preferred direction of the needles are either parallel—as in perfectly cleaved case—or twisted around 120° [3]. Fig. 5 gives an AFM image of a $100 \times 100\,\mu m^2$ area which has a cleavage step through the whole scanning area. The step is a clear border which separates areas with different needle directions. The alignment of the needles is rotated at an angle of 120° between the terraces. The needle morphology on different terraces, however, remains identical. Optical microscopy is employed to determine different needle directions relative to the substrate. These experiments reveal the astonishing result that there exist only two preferred needle directions twisted around 120°. To explain this behaviour it is required to investigate the crystalline structure of mica.

The used mica substrates are $2M_1$-muscovite with the formula unit $KAl_2(AlSi_3)O_{10}(OH,F)_2$. The lattice constants are $a = 5.20\,\text{Å}$, $b = 9.03\,\text{Å}$, $c = 20.11\,\text{Å}$, $\alpha = 90.00°$, $\beta = 95.78°$, $\gamma = 90.00°$. The muscovite structure is a stacked sandwich structure as depicted in Fig. 6a, where three sandwich layers are displayed (a detailed description can be found in Ref. [9]). Each sandwich layer is built of three intralayers. At first there are silicate sheets which are composed of (SiO_4) tetrahedrons. These tetrahedrons are linked laterally with adjacent tetrahedrons by sharing 3 corners each which results in the typical pseudo-hexagonal structure of mica. The remaining unshared corners are directed in the same direction. In the upper part of Fig. 6a, Si and O atoms are indicated as medium and small black spheres,

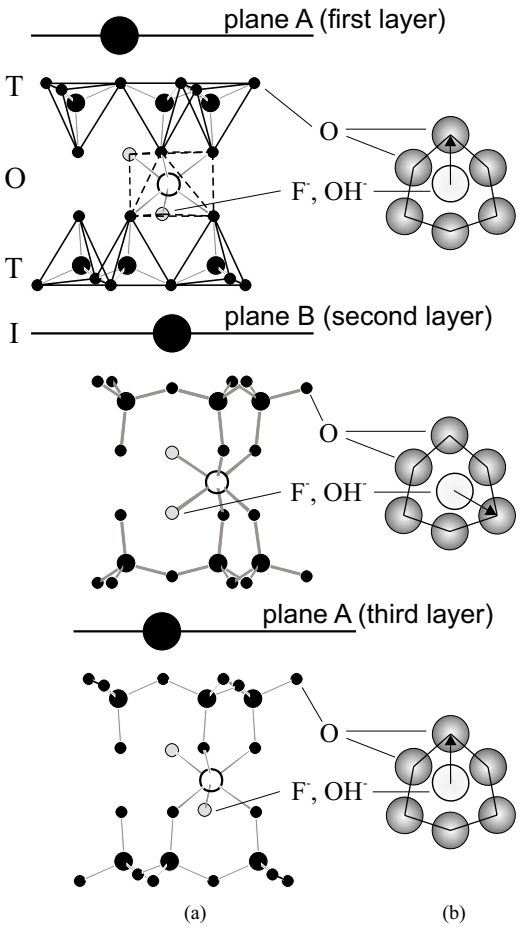

Fig. 6. (a) Crystal structure of mica (muscovite) in a view parallel to the crystallographic (0 0 1) plane of mica. The displayed atoms are potassium (large filled circles), silicon (medium filled circles), oxygen (small filled circles), aluminium (open circles), (OH^-, F^-) anions (light grey circles). (b) Surface arrangements of the uppermost oxygen layer. The inner atoms represent the lower located anions. All atoms are displayed with van der Waals spheres. The arrows indicate the shift of dislocation from the centre of the pseudo-hexagonal opening. Each arrangement corresponds to the cleavage planes given in (a).

respectively. The tetrahedron structures are also indicated as solid lines. In each sandwich layer there are two of these tetrahedral silicate layers (T) which are oriented with their unshared corners towards each other – also visible in Fig. 6a. The two silicate layers sandwich small ions like aluminium which are octahedrally coordinated (O). However, the inward directed corners of the silicate layers occupy only six of the required eight atom positions of the O layer. Hence, other anions like flour or hydroxyl are built in. In Fig. 6a, the aluminium and the additional flour atoms are indicated as open and grey spheres, respectively. The octahedrons are represented by dashed lines. These T–O–T sandwiches are stacked with interlayers (I) consisting of potassium atoms. This interlayer is needed to balance the formula due to the substitution of Si^{+3} atoms by Al^{+4} atoms in each T layer. The potassium atoms are indicated as large black spheres in Fig. 6a. Due to the low interaction between the I and the T–O–T layer the crystal is easy to cleave along this plane which is identical with the crystallographic (0 0 1) plane of muscovite. These planes are indicated as solid lines in Fig. 6a, which are also denoted as plane A and plane B. It can be noted that the used substrate is also cleaved along this crystallographic plane. However, adjacent sandwich structures are not arranged exactly upon each other. As is visible in Fig. 6a, there exist only two slightly different surface arrangements of cleavage planes (plane A and plane B) which need to be considered.

Since the oxygen atoms of the T layer represent the top atoms of mica (0 0 1) cleavage surfaces (see Fig. 6a), these oxygen layers have to be considered for interactions between PSP molecules and the substrate. As a result of charge repulsion in the O layer the ideal hexagonal surface of the oxygen is remarkably distorted [9]. The result is a three-fold symmetry of the entire surface formed by the oxygen atoms. Fig. 6b shows the distorted surface formed by the oxygen atoms (referred to the corresponding oxygen atoms in Fig. 6a) in which the three-fold symmetry is clearly visible. Each surface arrangement corresponds to the cleavage plane A or B in Fig. 6a. The oxygen atoms are displayed by dark grey spheres with their van der Waals spheres. In the centres of the hexagons—the so-called hexagonal openings—the anions are also displayed, although they are located in the octahedral layer below (also referred to the corresponding anions in Fig. 6a). As a result of the charge repulsion within the O layer the anions (OH^-, F^-) are dislocated from the centre of the hexagonal openings—which leads to the two-fold symmetry of mica (0 0 1) surfaces. It is evident

from Fig. 6 that the actual difference between two adjacent cleavage planes of muscovite is just the dislocation direction of the anions. Moreover, it is clear that there are only two different shift directions of the anions and they are twisted by 120°. It can be noted that a cleavage plane with a third direction of shift—twisted another 120°—does not exist. It can also be noted that the considerations above are based on the bulk structure of muscovite. Computer simulations of the (0 0 1) muscovite surface, however, reveal no remarkable differences compared with the mentioned results [10].

The experimental results reveal that PSP crystallites show two different needle directions on different terraces of mica (0 0 1) which are separated by cleavage steps. The twist angle between the needle directions is found to be 120° and a third direction—another 120°—could not be observed. The surface arrangements of different cleavage planes of mica (0 0 1) show a similar behaviour in terms of the dislocation direction of the lower located anions (OH^-, F^-). Therefore, we conclude that the growth of the PSP crystallites is influenced by these anions.

After the cleavage process of mica the remaining potassium atoms are not ideally distributed [12]. Since these atoms act as charge compensations between adjacent T–O–T layers the cleaved mica (0 0 1) surface is partially negatively charged. The contacting H atoms of PSP molecules, on the other hand, are slightly positively charged ($\sim +0{,}15$.e) as a result of a charge shift towards the carbon atoms [11]. Therefore, electrostatic interactions between the PSP molecules and the mica surface could be responsible for the actual binding.

4. Conclusion

Epitaxial growth of PSP is observed on freshly cleaved mica (0 0 1). AFM measurements reveal a needle-like morphology which reflects the monoclinic symmetry of mica (0 0 1). At cleavage steps the needle direction can either keep the same direction or change their orientation by 120°. No third needle direction is observed. The epitaxial relation between PSP and substrate is characterised by XRD-PF. The interactions between PSP molecules have been found to be stronger than the interactions between PSP and mica. Investigations of mica (0 0 1) cleavage planes reveal that adjacent cleavage planes twist their surface geometry also around 120°. A third direction is also missing which has the identical behaviour of PSP needle directions in case of not perfectly cleaved mica surfaces.

References

[1] M. Era, T. Tsutsui, S. Saito, Appl. Phys. Lett. 67 (1995) 2436.
[2] H. Yanagi, T. Moorikawa, Appl. Phys. Lett. 75 (1999) 187.
[3] A. Andreev, G. Matt, C.J. Brabec, H. Sitter, D. Badt, H. Seyringer, N.S. Sariciftci, Adv. Mater. 12 (2000) 629.
[4] A. Andreev, H. Sitter, C.J. Brabec, P. Hinterdorfer, G. Springholz, N.S. Sariciftci 116 (2001) 235.
[5] H. Plank, R. Resel, S. Purger, J. Keckes, A. Thierry, B. Lotz, A. Andreev, N.S. Sariciftci, H. Sitter, Phys. Rev. B 64 (2001) 235423.
[6] W. Kraus, G. Nolze, J. Appl. Crystallogr. 29 (1996) 301.
[7] K.N. Baker, A.V. Fratini, T. Resch, H.C. Knachel, W.W. Adams, E.P. Socci, B.L. Farmer, Polymer 34 (1993) 1571.
[8] S. Forrest, Chem. Rev. 97 (1997) 1793.
[9] S.W. Bailey, Structures of Layer Silicates, in: G.W. Brindley, G. Brown (Eds.), Crystal structure of Clay Minerals and their X-ray Identification, Mineral Soc. Monograph No. 5, London, 1980.
[10] M. Odelius, M. Bernasconi, M. Parrinello, Phys. Rev. Lett. 78 (1997) 2855.
[11] D.E. Williams, T.H. Starr, J. Comput. Chem. 1 (1977) 173.
[12] P.A. Campbell, L.J. Sinnamon, C.E. Thompson, D.G. Walmsley, Surf. Sci. 410 (1998) L768.